IOP Conf. Series: Materials Science and Engineering **161** (2016) 012061 doi:10.1088/1757-899X/161/1/012061

Behaviour of a ZnO thin film as MSG for biosensing material in sub-wavelength regime

Iftimie N[1], Steigmann R[1,2], Danila N A[1], Iacomi F[2], Faktorova D[3] and Savin A[1]

[1] Nondestructive Testing Department, National Institute of R&D for Technical Physics, Iasi, Romania
[2]Faculty of Physics, Alexandru Ioan Cuza University, Iasi, Romania
[3]Faculty of Electrical Engineering, University of Žilina, Žilina, Slovak Republic

Email: niftimie@phys-iasi.ro

Abstract. Zinc oxide nanostructured materials, such as films and nanoparticles, could provide a suitable platform for development of high performance biosensing material due to their unique fundamental material properties. In this study, the enzyme biosensing consisting of a zinc oxide (ZnO) nanoparticles were grown on SiO_2/Si substrates by vacuum thermal evaporation method and their sensing characteristics are examined in air and investigated. The film morphology is characterized by X-ray diffraction (XRD) the film crystalline quality and by scanning electron microscopy (SEM). Also, the interest in surface waves appeared due to evanescent waves in the metallic strip grating structure (MSG-Ag/ZnO/SiO_2/Si) in sub-wavelength regime. Before testing the sensor with metamaterials (MMs) lens in the sub-wavelength regime, a simulation of the evanescent wave's formation has been performed at the edge of Ag strips, with thicknesses in the range of micrometers.

1. Introduction

The stability of ZnO nanostructures under physiological conditions, being important for sensing and biosensing applications, depends on the crystal quality of the nanostructures but can be assumed as sufficient for structures grown by thermal evaporation methods [1]. Nanostructures made of ZnO are easy and reliable to produce in a wide manner of different forms and structures [2]. ZnO is very versatile and due to its high coupling coefficient, many applications exist, like Surface Acoustic Wave (SAW) devices [3], bulk acoustic wave devices, gas sensors [4-5], infrared detectors, tactile sensor arrays and enzyme biosensors [6]. The evidence of plasmons apparition in structures of wires with micrometric diameters has been shown for Al at frequency of 8.2 GHz [7].

The possibility to excite plasmons at lower or equivalent frequencies in complex structures containing silver metallic strip gratings (MSGs) was investigated. A MSG interface supports the well-known surface plasmon-polariton (SPP) modes, yielded by the coupling of the EM field with the coherent oscillations of the free electrons in the metal. Their ability to store and propagate the EM energy at subwavelength scales is essential for many applications such as biosensing, photonic circuits and optical data storage.

In this paper, in order to confirm the availability of ZnO nanostructures for convenient high-efficiency biosensors, the glucose sensing performance via the electrical properties to be measured in

air was investigated. Also, the interest in surface waves appeared due to evanescent waves in the MSG in sub-wavelength regime. The experimental test is making with the sensor with metamaterials lens [8,9] in the sub-wavelength regime, and a simulation of the evanescent wave's formation has been performed at the edge of Ag strips, with thicknesses in the range of micrometers. In this work, high quality ZnO films were grown on SiO_2/Si substrates by vacuum thermal evaporation method is characterized by X-ray diffraction the film crystalline quality and by Scanning Electron Microscopy (SEM) the film morphology. This method has many advantages such as being a low cost, simple, high yield, 10^{-5} Torr pressure, deposition rate of 0.05 mm/s and a deposition time of 30 s. The high electrochemical response can be attributed to the unique structural properties of our sensor electrode like the high surface to volume ratios of ZnO nanoparticles, which can provide a favorable microenvironment for the immobilization of uricase enzyme and retain the good enzymatic activities which in turn enhances the sensitivity of sensor electrode for the analyte, as demonstrated by the detection of uric acid in the absence of a mediator.

2. Experimental section

The morphology of the nanostructure significantly affects its electrochemical properties, so numerous ZnO nanostructures have been investigated for application in enzyme biosensor. The physical, chemical and surface properties of the desired support determine the method of uricase enzyme immobilization, the nature of the immobilized sensing molecules, and the overall biosensor performance. While the redox capabilities of enzymes are not typically enhanced because of their insulated redox centers, specific ZnO nanostructures can facilitate direct electron transfer (DET) between enzyme electroactive sites and external electrodes [10-14]. The synthesis of ZnO nanostructures by different techniques has promoted the fabrication of enzyme biosensors.

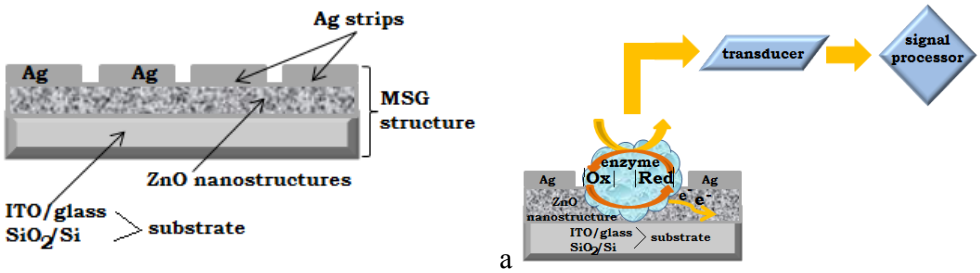

Figure 1. a) MSG structure; b) Working principles of a ZnO nanostructure-based enzyme biosensing.

To sensing mechanism for enzyme biosensing (e.g. uric acid and ascorbic acid) designed in this purpose, the voltage applied across the two electrodes causes a current to flow via electron tunneling through the potential barriers between nanoparticles. Detecting uric acid in physiological fluids is important for diagnosing disorders associated with altered purine metabolism [15,16]. Equation (1) describe the uricase catalyzing reaction:

$$C_5H_4N_4O_3(\text{uric acid}) + O_2 + 2H_2O \xrightarrow{uricase} C_5H_6N_4O_3(\text{allantoin}) + CO_2 + H_2O_2 \quad (1)$$

A reagentless uric acid biosensor based on uricase functionalized ZnO nanostructures exhibits good thermal stability and anti-interference capability. When uric acid is oxidized in the presence of uricase it is turned into allantoin along with carbon dioxide and hydrogen peroxide. Due to the presence of water (H-OH), it is a high probability that allantoin will accept a proton from (H-OH) converting it to allantoinium ion, which in turn will interact with the ZnO nanostructures and produce a potential change at the electrode. As the concentration of ions changes in surrounding the ZnO nanostructures and the electrode potential will change. The potentiometric responses of the sensor electrodes were studied in uric acid solutions made in buffer (PBS pH 7.0).

3. Structural characterization

The XRD patterns of the obtained structures were carried out on a diffractometer using CuKα radiation (λ =1.5406 Å) (Figure 2). The samples were analyzed in the range of 2θ=5°÷80° with a scanning angle rate of 0.02 and a 2 s/step count time. The experimental XRD patterns were identified using Crystallographica Search-Match programme. The XRD peaks for ZnO crystalline phases are visible. The reflection peaks, at (100), (002), (101), (110), (103) and (112) were indicative of the hexagonal wurtzite ZnO nanostructure.The ZnO film is polycrystalline in nature having a preferred grain growth orientation along (002) and (101) planes which correspond with the peaks at 34.4 and 36.2°. The weakness of the peaks is related to the thickness of the thin films. This is due the nature of the source material and it is assumed that only nanoparticles migration from the source to the substrate takes place.

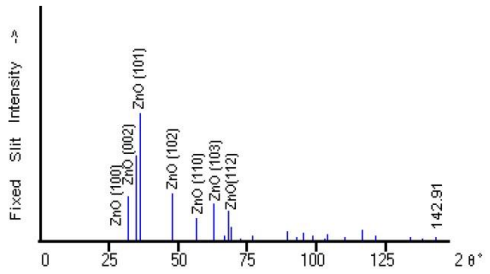

Figure 2. XRD ZnO thin film deposited on SiO_2/Si substrate.

For structural characterization of Ag/ZnO/substrate nanostructures scanning electron microscopy, SEM, investigations were performed. The SEM showed that the structure of the films of ZnO is columnar (Figure 3 a). It can be shown also that of ZnO nanostructured without bound enzyme had a uniform film, while ZnO nanostructured with bound enzyme had many globular structures. These observations confirmed immobilization of enzyme. The surfaces are without inclusions and defects, fact that make them appropriate for radio frequencies applications.

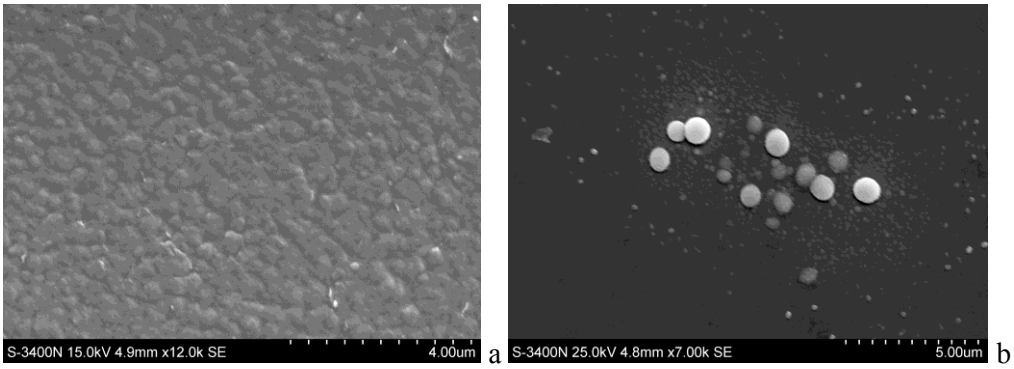

Figure 3. The SEM images of cholesterol oxidase bound ZnO nanostructures: (a) without enzyme; (b) with immobilized uricase

4. Evanescent waves. FDTD simulation

Due to experimental difficulties in obtaining a perfect lens, the manipulation of evanescent modes can be made with an electromagnetic sensor with MMs lenses that have, at the operation frequency, either μ_{eff} = -1, and the lens can focus magnetic evanescent modes [18-20,9,21-23]. The spatial resolution of the system was verified according to [20] and the analysis of data obtained show that the realization of MM lenses in the radiofrequency range is possible using CSR, whose distortions are minimal and whose calculation are based on Fourier optic principles [24].

The sensor and experimental set-up is presented [25,17]. Generation and detection of evanescent waves in slits are made using the electromagnetic sensor lens. The rectangular frame used for the generation of TMz polarized waves is identical with rectangular frame used for the simulation model and the lens is made from a CSR [8,17]. The working frequency was 474 MHz. The simulation was make using XFDTD 6.3 software produced by REMCOM [26]. In Figure 4 is shown the result of simulation with XFDTD. The E_y component, which counts in our case, is displayed. In [27] it has been presented the behavior of the field with air in the slits, it can be shown that, for uricase between the strips, the amplitude of the electric field has the same behavior as in [22] but the amplitude decreasing due to electrical permittivity high of the uricase. Thus, the symmetrical maxima appear in the middle of the slits, decreasing to the minimum value, on the strips edges. Inside the strips, other pair of maxima appears, followed by the decreasing to middle of the strip.

The Fig. 6 shows the dependency of voltage amplitude induced in the reception coil of sensor at the scanning of the MSG taken into study, the image showing that the type of sensor allows the correct emphasizing of extremely thick conductive strips and eventual interruptions.

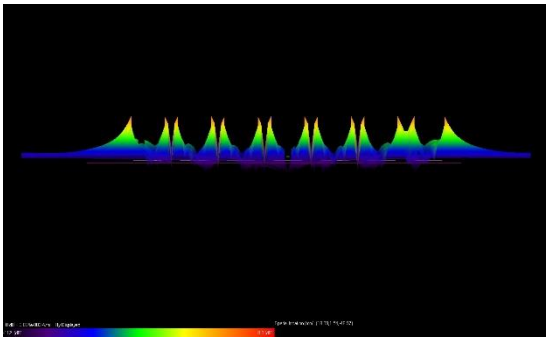

Figure 4. Numerical results for electric-field amplitude distribution near the strips; the field values are normalized to the amplitude of the incident field.

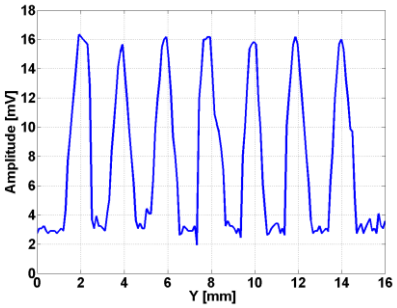

Figure 5. Amplitude of voltage induced in the reception coil at the scanning of silver strip grating.

The existence of a single evanescent mode, theoretically foreseen, is experimentally confirmed by the existence of a local maximum in the middle zone of the slits, followed by an accentuated decreasing on the edge of the strips. The results are in good concordance with theoretical estimations, that confirms good adhesion of silver on $ZnO/SiO_2/Si$, also good alignments of strips.

5. Experimental set-up and biosensing properties

ZnO nanostructured have excellent prospects for interfacing biological recognition events with electronic signal transduction as a new generation of biosensors in which active enzymes sites are coupled directly with a nanostructured ZnO electrode resulting in direct electron transfer between the enzyme and nanostructured ZnO with improved biosensing properties.

The initial experimental dates were carried out using a multimeter device because of its versatility in measuring resistance, voltage and ampere. The multimeter probes were immersed into 5 ml sodium phosphate buffer (0.02 M, pH 7.0) in a beaker. The reaction was started by adding 0.5 ml of enzyme solution. Based on the current produced during the chemical reaction the number of molecules of uricase and consequently the amount of uricase present in the sample could be determined. The current was measured at varying concentrations of uricase to obtain a full working range. The sensing mechanism of most electrochemical uric acid sensors is based on an enzymatic reaction catalyzed by uricase as described in Figure 6.

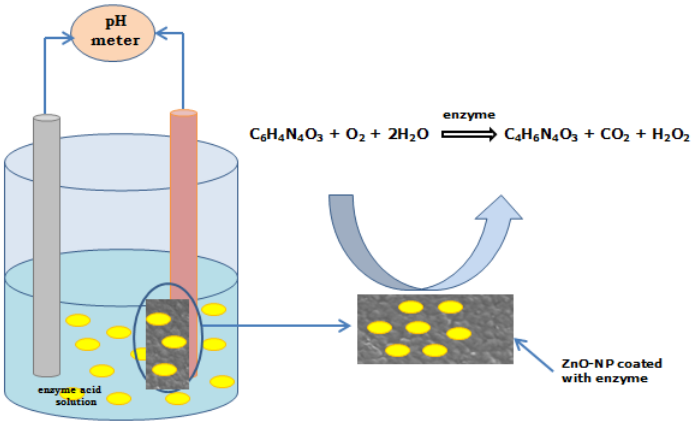

Figure 6. Schematic diagram of the uric acid sensing setup using ZnO-NP coated with uricase as working electrode showing the possible electrochemical reaction near the working electrode.

To study effect of uricase concentration, the concentration was varied from 100 to 1300 mg/dl and amperometric measurements were made after 0.5 ml of uric acid added. The probe was immersed into the solutions and the displayed ampere was noted against the concentration of the solution.

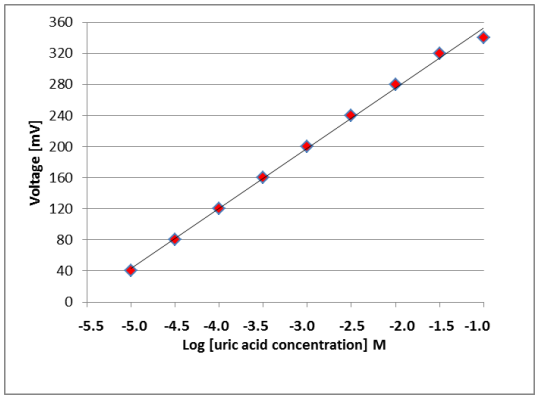

Figure 7. The calibration curve of uric acid biosensor based on $ZnO/SiO_2/Si$ nanostructures for linear concentration range of 5.2 to 20.8 mM

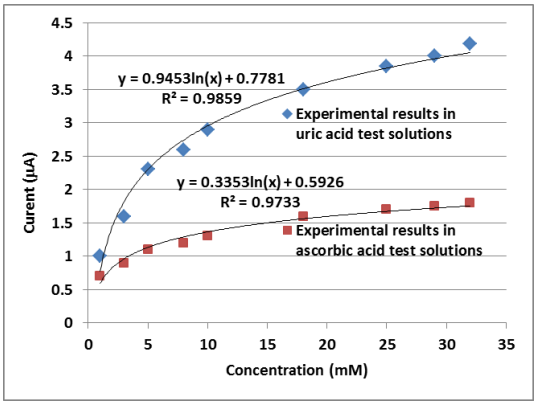

Figure 8. Variation in the current at a fixed potential of 0.04 V with changing uricase concentration to $Ag/ZnO/SiO_2/Si$ architecture biosensing

Figure 7 shows the relation between the output potential response and uricase concentration for the element biosensing. It is clearly seen from the graph that the response current increases as the concentration of uricase increases and saturated at high concentration of uricase which suggests the saturation of active sites of the enzymes at those uric acid levels. The selectivity study suggests that the presence of interferants, like ascorbic acid, have a negligible effect on the performance of the $Ag/ZnO/SiO_2/Si$ architecture toward sensing of uricase (Figure 8). The calibration curves were obtained in the range of 100-1300 mg/dl (2.6-33.8 mM), with coefficient of determination was estimated to be $R^2 = 0.9859$. Under optimized conditions, the steady-state current showed a linear dynamic range of 200-800 mg/dl (5.2-20.8 mM).

6. Conclusions

A simple fabrication technique for a biosensing electrochemical uric acid sensor based on ZnO nanostructures deposited on SiO_2/Si substrate by vacuum thermal evaporation was performed. The Ag strip grating thickness of µm order is comparable with the depth penetration of electromagnetic wave of

474 MHz, so that evanescent waves appear at the edge of strips and their manipulation can improve the resolution power of the sensor.

The experimental measurement was made with a sensor with metamaterials lens. It has been proved that sensors with metamaterials lens can be used in amplitude evaluation of the evanescent waves formed at the edge of strips of $Ag/ZnO/SiO_2/Si$ structure. The calibration curves were obtained in the range of 2.6 to 33.8 mM, with coefficient of determination was estimated to be $R^2 = 0.9859$. By results obtained it is shown that the element biosensing structure investigated is rapid and sensitive for the detection of uricase. One can concluded that due to the simple synthesis and electrode fabrication, good sensitivity, low detection limit and fast response, the ZnO nanostructured opens a way for the fabrication of highly efficient cholesterol biosensors.

References

[1] Zhou J, Xhu N S and Wang Z L 2006 Dissolving behavior and stability of ZnO wires in biofluids: a study on biodegradability and biocompatibility of ZnO nanostructures *Adv. Mater.* **18** 2432-2435

[2] Wang Z L 2004 Zinc oxide nanostructures: growth, properties and applications *J. Phys. Condens. Matter.* **16** 829-858

[3] Fu Q, Deng J, Zhou D, Gong S, Zhong S and Luo W 2012 *IMCS 2012 – The 14th International Meeting on Chemical Sensors* 905-908

[4] Rambu A P, Tiron V, Nica V and Iftimie N 2013 Functional properties of ZnO films prepared by thermal oxidation of metallic films *J. Appl. Phys.* **113** 234506-6

[5] Iftimie N, Iacomi F and Rezlescu N 2008 High performance gas sensing materials based on nanostructured zinc oxide films *Journal of Optoelectronics and Advanced Materials* **10** 1810–1813

[6] Faktorova D 2010 Dielectric spectroscopy of glucose turnover in cancerous tissue model *In: Acta Technica CSAV* **55** (1) 29-37

[7] Pendry J B, Holden A J, Stewart W J and Youngs I 1996 Extremely Low Frequency Plasmons in Metallic Mesostructures *Phys. Rev. Lett.* **76** 4773-4776

[8] Grimberg R, Savin A, Steigmann R, Serghiac B and Bruma A 2011 Electromagnetic non-destructive evaluation using metamaterials *INSIGHT* **53** (3) 132-137

[9] Savin A, Steigmann R, Bruma A and Sturm R 2015 An electromagnetic sensors with a metamaterial lens for nondestructive evaluation of composite materials *Sensors* **15** 15903-15920

[10] Zhao Y, Yan X, Kang Z, Lin P, Fang X, Lei Y, Ma S and Zhang Y 2013 Highly sensitive uric acid biosensor based on individual zinc oxide micro/nanowires *Microchim. Acta.* **180** (9) 759–766

[11] Liu J, Guo C, Li C M, Li Y, Chi Q, Huang X, Liao L and Yu T 2009 Carbon-decorated ZnO nanowire array: a novel platform for direct electrochemistry of enzymes and biosensing applications *Electrochem. Commun.* **11** 202–205

[12] Dai Z, Shao G, Hong J, Bao J and Shen J 2009 Immobilization and direct electrochemistry of glucose oxidase on a tetragonal pyramid-shaped porous ZnO nanostructure for a glucose biosensor *Biosens. Bioelectron.* **24** (1) 286–1291

[13] Kavitha T, Gopalan A I, Lee K P and Park S Y. 2012 Glucose sensing, photocatalytic and antibacterial properties of graphene–ZnO nanoparticle hybrids *Carbon* **50** (8) 2994–3000

[14] Jafari M, Khodadadi A A, Mortazavi Y and Ghorchian H 2012 *IMCS 2012—The 14th International Meeting on Chemical Sensors* 687–689

[15] Usman Ali S M, Alvi N H, Ibupoto Z, Nur O, Willander M and Danielsson B 2011 Selective potentiometric determination of uric acid with uricase immobilized on ZnO nanowires *Sensors and Actuators B* **152** 241–247

[16] Zhang Y, Kang Z, Yan X and Liao Q 2015 ZnO nanostructures in enzyme biosensors, *Sci. China. Mater.* **58** 60–76

[17] Steigmann R, Iftimie N and Savin A 2015 Characterization of the Thin Films Structures in Subwavelength Regime as Biosensing Materials *Applied Mechanics and Materials: Advanced Research in Aerospace, Robotics, Manufacturing Systems, Mechanical Engineering and Bioengineering* **772** 62-66
[18] Pendry J B, Holden A J, Stewart W J and Youngs I 1996 Extremely Low Frequency Plasmons in Metallic Mesostructures *Phys. Rev. Lett*. **76** 4773-4776
[19] Pendry J B, Holden A J, Robbins D J and Stewart W J 1999 Magnetism from conductors and enhanced non-linear phenomena *IEEE Trans. Microw. Theory Tech*. **47** 47-58
[20] Gribic A and Eleftheriades G V 2003 Growing evanescent waves in negative-refractive-index transmission-line media *Applied Physics Letters* **82**(12) 1815-17
[21] Grimberg R and Tian G Y 2012 High-frequency electromagnetic non-destructive evaluation for high spatial resolution, using metamaterials *Proc. R. Soc. A*, **468** 3080–3099
[22] Savin A, Steigmann R and Bruma A 2014 Metallic Strip Gratings in the Sub-Subwavelength Regime *Sensors* **14**(7) 11786-11804
[23] Savin A and Steigmann R, 2014 *patent RO129801-A0/2014*, Electromagnetic sensor for assessing integrity of braids of single-layer printed wiring on flexible support and of layered meso-structures
[24] Born M and Wolf E 1999 *Principle of Optics* 7th ed. (Cambridge: Cambridge University Press)
[25] Grimberg R 2013 Electromagnetic metamaterials *Mater. Sci. Eng. B* **178** 1285–1295
[26] Lagendijk A, Van Tiggelen B and Wiersma D S 2009 Fifty years of Anderson localization *Physics Today* **62**(8) 24-29
[27] Iftimie N, Tascu S, Salaoru I, Steigmann R, Savin A, Irimia M and Iacomi F 2015 The evanescent waves in metallic strip gratings and complex structures in subwavelength regime *Materials Today: Proceedings*, **2**(10) 3486-3452

Acknowledgments
This paper is supported by Romanian Ministry of National Education under project PN-II-ID-PCE-2012-4-0437 and Nucleus Program PN 16 37 01 01.